European Journal of Pharmaceutics and Biopharmaceutics 135 (2019) 49–60

Contents lists available at ScienceDirect

European Journal of Pharmaceutics and Biopharmaceutics

journal homepage: www.elsevier.com/locate/ejpb

Research paper

Managing active pharmaceutical ingredient raw material variability during twin-screw blend feeding

F. Stauffer[a], V. Vanhoorne[b], G. Pilcer[c], Pierre-François Chavez[c], M.A. Schubert[c], C. Vervaet[b], T. De Beer[a,*]

[a] Laboratory of Pharmaceutical Process Analytical Technology, Ghent University, Ghent, Belgium
[b] Laboratory of Pharmaceutical Technology, Ghent University, Ghent, Belgium
[c] Drug Delivery Design and Development, UCB, Braine l'Alleud, Belgium

ARTICLE INFO

Keywords:
Material properties
Managing active pharmaceutical ingredient variability
Multivariate data analysis
Quality by design
Continuous manufacturing
Twin-screw feeding

ABSTRACT

Continuous powder feeding is a critical step in continuous manufacturing of solid dosage forms, as this unit operation should ensure the mass flow consistency at the desired powder feed rate to guarantee the process throughput and final product consistency. In this study, twin-screw feeding of a pharmaceutical formulation (i.e., blend) existing of a highly dosed very poorly flowing active pharmaceutical ingredient (API) leading to insufficient feeding capacity was investigated. Furthermore, the API showed very high batch-to-batch variability in raw material properties dominating the formulation blend properties. Formulation changes were evaluated to improve the flowability of the blends and to mitigate the impact of API batch-to-batch variability on the twin-screw feeding. Herewith, feeding evaluation tests and an extensive material characterization of the reformulated blends were performed to assess the impact of the formulation changes upon continuous twin-screw feeding. The transfer of the glidant from extra-granular to intra-granular phase allowed to improve the flowability of the blends. A sufficient feeding capacity for the downstream process and a mitigation of the impact of batch-to-batch variability of the API upon twin-screw feeding of the blends could be achieved. No effect of the formulation or of the API properties on the feeding stability was observed. The material characterization of the blends allowed identifying the material attributes which were critical for continuous twin-screw feeding (i.e., bulk density, mass charge and powder cohesiveness).

1. Introduction

In recent years, continuous manufacturing gained more and more interest within the pharmaceutical industry [1–5]. The main drivers to apply continuous manufacturing are the cost reduction, the regulatory encouragement and the potential improved quality guarantee of the final product [3,4]. The shift to continuous manufacturing nonetheless implies new technical and scientific challenges, such as cleanability, start-up and shut-down procedures, powder handling, material tracking and in-process measurements [2]. The quality assurance relies on the ability of the process to remain in state of control and to produce a product with consistent critical quality attributes (CQAs). Understanding raw material variability and unit operation variances and how they propagate through the process is crucial to ensure the final product consistency. In case of continuous feeding, process variances such as inconsistent mass flow or changes in feeding capacity can be induced by poorly flowable powders, raw material variability and/or hopper refilling. Such feeding variances can impact the content uniformity in continuous blending [6,7], the particle size and density of the granules formed during subsequent twin screw granulation [8] or the extrusion stability [9] during downstream processing.

As first unit operation in continuous pharmaceutical manufacturing lines for solid dosage forms, appropriate powder feeding is crucial to ensure targeted and consistent throughput and final product consistency. To evaluate and consequently achieve suitable feeding operation performance, Engisch et al. proposed a methodology to characterize loss-in-weight feeders using an external catch scale to accurately measure the feeding capacity (i.e., maximum mass flow achievable) and stability (i.e., mass flow consistency) [10]. This method was applied to select appropriate feeders and tooling for different types of powder [10,11] and to evaluate feeder stability during refilling stages [12]. This approach is well suited to empirically determine the optimal feeding conditions for a certain material. However, it is well known that feeding performance is strongly impacted by powder properties [10,11,13] and hence this feeder characterization should be performed for each new material. Freeman et al. tried to correlate the

* Corresponding author.

https://doi.org/10.1016/j.ejpb.2018.12.012
Received 30 March 2018; Received in revised form 31 October 2018; Accepted 20 December 2018
Available online 22 December 2018

feeding capacity of two feeders with powder flowability characteristics measured using FT4 [14]. However, also other powder properties than the ones that can be determined with the FT4 (e.g., angle of avalanche, electrostaticity) have an impact on feeding [15]. Therefore, a few other studies correlated more powder physical properties such as particles size, shape, Hausner ratio, compressibility ratio, angle of repose and flow to feeding performance using multivariate data-analysis [16,17]. These studies are useful examples in terms of methodology, but their conclusions strongly depend on the range of selected powders and powder characteristics. For instance, conclusions made for a large range of relatively well flowing pharmaceutical excipients do not apply for cohesive Active Pharmaceutical Ingredients (API) [18]. Feeding performance may also be impacted by raw materials batch-to-batch variability. A significant impact of the raw material variability was indeed reported for high shear granulation [19,20], twin-screw granulation [21,22], roller compaction [23,24] or tableting [25,26], but not yet for continuous feeding. Continuous feeding of raw material is indeed envisaged within a continuous manufacturing process. It is however not always possible to achieve required feeding and blending performances for all raw materials. Certain APIs and lubricants are particularly difficult to feed due to their high cohesiveness [11,18]. For high drug-load formulations, the restrictions in terms of appropriate raw material feeding capacity can become a limiting factor for the process throughput. In such case, a prior batch blending process could be envisaged as an alternative to achieve desired feeding throughput in the continuous line. In the latter scenario, blends should also demonstrate sufficient stability to avoid segregation during refilling stages. Additionally, the formulation should allow mitigating the impact of eventual API batch-to-batch material property variability, especially for highly drug loaded formulations.

The study described in this article was performed in the context of the process transfer from batch high-shear granulation to continuous twin-screw wet granulation of a commercial product. The product was a tablet formulated with 41.7% (w/w) of a very cohesive API, representing 65% (w/w) of its intra-granular phase. The considered production throughput requested a consistent mass flow of 16 kg/h of API. As the API exhibited very poor flowability, preliminary tests on the considered production line showed the impossibility to achieve a sufficient API mass flow. Feeding of a batch-wise prepared formulation blend was therefore needed. The API properties (e.g., PSD, density, surface energy, flowability) varied largely from batch to batch [27]. A dominant influence of the API batch upon feeding performance of the formulation blend was expected because of the high drug-load. The aim of this study was therefore to improve the feeding capacity of the formulation blend and to mitigate the impact of the API batch-to-batch variability on the feeding of the formulation blend. Herewith, changes in feeder design and in formulation composition were considered. However, the industrial context of the study restricted the range of feasible formulation changes and feeding configurations. Considering the feeder design, the setup selection was limited to the available equipment and tooling for the envisaged continuous production line. The current study therefore focused on formulation optimization. Screening and optimization of alternative formulations were performed on small scale. Feeding trials were then performed to compare feeding performance and API batch-to-batch variability mitigation obtained with the original and optimized formulation.

2. Material and methods

2.1. Materials

2.1.1. API batches

Eight different API batches were used to study the impact of the API batch-to-batch variability on continuous feeding. The physical properties of the API and its batch-to-batch variability were described in detail in a previous paper of the authors [27]. The studied API is produced via four different synthesis, crystallisation, drying and delumping routes. Process 1 (route 1) is a non-seeded uncontrolled crystallization process followed by paddle drying and sieving. Process 2 is identical to process 1 except that the crystallization is seeded. Process 3 uses another synthetic route and different crystallization and drying processes. Crystallization is herewith also seeded. Process 4 is an ultrasound-assisted crystallization (sonocrystallization) performed at the development stage only. The used API batches in this study were produced at full commercial scale – except for the APIs processed via process 4. The batches were labelled according to their production process (P1-4) and batch number (/1-3): P1/1-2, P2/1-3, P3/1 and P4/1-2. All eight batches were within the specifications in terms of purity, residual solvents, crystallinity and polymorphism.

2.1.2. Formulation

The formulation contained 41.7% (w/w) of API, 11.7% (w/w) of microcrystalline cellulose (Avicel® PH102, FMC Biopolymer, Philadelphia, USA) as filler, 10.4% (w/w) of hydroxypropyl cellulose low substituted (L-HPC LH21, ShinEtsu, Wiesbaden, Germany) as dry binder, 0.8% (w/w) of hydroxypropyl cellulose (Klucel-LF, Ashland, Rotterdam, the Netherlands) as wet binder, 26.1% (w/w) of silicified microcrystalline cellulose (SMCC, Prosolv HD90, JRS Pharma, Rosenberg, Germany) as filler, 8.3% (w/w) of crospovidone (Kollidon CL, BASF, Ludwigshafen, Germany) as disintegrant and 1.0% (w/w) of magnesium stearate (Ligamed MF, Peter Greven, Venlo, the Netherlands) as lubricant. The intra-granular phase of the original batch wise processed formulation only contained the API, microcrystalline cellulose and hydroxypropyl cellulose low substituted (F1 in Table 1).

2.2. Formulation development

In order to improve blend flowability and to mitigate the impact of API batch-to-batch variability on continuous feeding performance and stability, formulation changes were evaluated.

Formulation development was performed in three steps: (i) a formulation screening (referred to as "**screening study**"), (ii) an optimization of the selected formulation (referred to as "**optimization study**") and (iii) tests on actual feeders (referred to as "**feeding study**").

The **screening study** aimed at selecting the best strategy of reformulation. As the studied product is already on the market only the incorporated excipients (intra-granular/extra-granular) could be modified. Therefore, slightly modified alternative formulations were tested in the **screening study**, and compared with the original formulation (F1) to improve the formulation blend flowability and feeding and to

Table 1
Screening study – composition of the evaluated formulations. "Intra": intra-granular phase. "Extra": Extra-granular phase. In bold: ingredients present in the evaluated formulation blends.

		Incorporation phase		
Ingredient	Proportion	F1	F2	F3
API	41.7%	**intra**	**intra**	**intra**
Microcrystalline cellulose	11.7%	**intra**	**intra**	**intra**
Hydroxypropyl cellulose low-substituted	10.4%	**intra**	**intra**	**intra**
Hydroxypropyl cellulose	0.8%	intra (wet)	intra (wet)	intra (wet)
Colloidal silicon dioxide	0.5%	extra (SMCC)	**intra (SMCC)**	**intra**
Microcrystalline cellulose	25.6%	extra (SMCC)	**intra (SMCC)**	extra
Crospovidone	8.3%	extra	extra	extra
Magnesium stearate	1.0%	extra	extra	extra

mitigate the impact of the API batch-to-batch variability. In formulation F2, the total amount of SMCC was transferred from the extra-granular phase to the intra-granular phase to dilute the API with a well flowable excipient. SMCC is composed of microcrystalline cellulose co-processed with colloidal silicon dioxide to reduce powder cohesiveness. In formulation F3, the colloidal silicon dioxide (Aerosil, Evonik, Antwerp, Belgium), originally present in the SMCC, was transferred to the intra-granular phase (but keeping MCC in the extra-granular phase – see Table 1). In summary, the original formulation (F1), a diluted formulation (F2) and a formulation with glidant (F3) were tested (Table 1). API batches having the largest possible raw materials differences were used to test the three formulations.

In the **optimization study**, the most flowable formulation selected in the screening study was further optimized regarding the formulation blend flowability. The total amount of excipients in the formulation was kept constant but their proportion between the intra-granular and extra-granular phases was modified. An external API batch was selected for the optimization study.

The formulation blends for the **screening and optimization studies** were produced at small scale (100 g) using a 1L high shear blender (4 M8, Procept, Zelzate, Belgium). Powders were introduced in the following order: Avicel PH102, API alone (F1) or pre-mixed with Prosolv HD90 (F2) or Aerosil (F3) and L-HPC. The impeller speed was set at 100 rpm for 15 min.

2.3. Feeding study

In the **feeding study**, the original and optimized formulation were prepared using eight different API batches presenting the largest range of known raw material variability. The formulation blends were produced at larger scale (5 kg) using a batch planetary blender (Collette MP20, GEA, Wommelgem, Belgium). Here, the impeller speed was set at 69 rpm for 15 min.

2.3.1. Feeders

Two loss-in-weight feeders were used during the feeding trials: a KT20 and a KT35 (Coperion K-tron, Switzerland, Table 2). The KT20 feeder was the feeder implemented in the Consigma 25 line that will be used for the processing of the formulation under study in this paper (GEA engineering, Wommelgem, Belgium). The KT35 is a larger scale feeder compared to the KT20 as it has larger screws and hopper volume. It was considered for the larger scale twin-screw granulation line (i.e., Consigma 50, GEA engineering, Wommelgem, Belgium) and is in this study also evaluated for potential future scale-up ambitions. Both feeders are composed of three parts: a volumetric twin screw feeder, a weighing platform and a gravimetric Proportional-Integral (PI) controller. Selection of the appropriate gear box, screws, agitator and screen are the first step of feeding development. This selection was performed during pre-tests and will not be outlined in this article. The gearbox controlling the screws was a type A combined with a motor with a maximum speed of 2000 rpm for both feeders. Coarse concave screws were selected to obtain the highest feeding capacity. A screen can be placed at the end of the feeder screws to improve the feeding stability. Due to the high electrostatic charge of the formulation blends, it was not possible to use a screen for this study.

2.3.2. Feeders evaluation

The feeder performance of the KT20 and KT35 was evaluated for the original formulation as well as for the optimized formulation with the different API batches.

2.3.2.1. Feeder capacity. The feeder capacity corresponds to the maximum powder feed rate (**PFR**) that a feeder can achieve for a certain powder. Engisch et al. [10] developed a standard procedure to evaluate the capacity of loss-in weight feeders by measuring the powder feed rate at increasing screw speeds. The feeding capacity can also be determined using the built-in auto feed factor calibration program of the feeder's controller. The feeding capacity is then extrapolated from a measurement of the powder feed rate at one intermediate screw speed. This option is faster, as only one screw speed is used, but can only be applied if the correlation between the feed rate and the volumetric screw speed is linear. As the linearity was assessed and confirmed during pre-tests with the investigated product, the feeding capacity was determined for both feeders with a screw speed set at 200 rpm in triplicate using the built-in feed factor calibration at a 100% hopper filling. The estimated max PFR was hence obtained.

2.3.2.2. Feeder stability. To evaluate the consistent target feed rate of 25 kg/h, a **stability** evaluation was performed by gravimetric feeding of the formulation blends at this target feed rate for about 30 min. An independent K-Sampler catch scale (Coperion K-tron, Niederlenz, Switzerland) was used during these trials to precisely measure the fluctuations in PFR as function of time. The powder was collected in a bucket placed below the outlet of the screws and positioned on the catch scale. In gravimetric control, the feeder interface pre-treated the feed rate data using a moving horizon estimation for each 30 s to reject the disturbances and increase the signal-to-noise ratio. This filtering procedure is well suited for process control, but is less appropriate to evaluate the stability of the feeding process. The catch scale allowed recording mass variations every 0.1 s. In the final envisaged continuous manufacturing process of the formulation under study, the feeder will be connected to a continuous twin-screw granulator with a typical residence time between 1 and 10 s [28]. In order to evaluate the feeding stability at a relevant frequency, the powder mass flow per second was used to calculate the standard deviation of the mass flow (**RSD**). Although refilling can affect the feeding stability [12], this aspect was not evaluated in the current study due to limitations in material availability. The impact of hopper refilling should nevertheless be investigated in further development trials.

2.4. Formulation blends characterization

The term powder “flowability” refers to a variety of powder behaviours (i.e., static, quasi-static and dynamic flowability). Flowability evaluation depends strongly on the measurement technique (e.g., angle of repose, angle of avalanche, ring shear test) as each equipment measures a certain type of behaviour [27,29]. To the best of the authors’ knowledge, there currently exists no scientific consensus about predictive material characterization tests reflecting the powder behaviour in twin-screw feeding. Most likely, a combination of material characterization techniques is needed. During the **screening** and **optimization studies**, blend characterization tests were limited to reduce the amount of material consumption. The ring shear test is commonly used for hopper designs and formulation development [30]. It was consequently selected in the **screening** and **optimization studies**. The cohesion index (CI) measured using the rotating drum was used in

Table 2
Feeder characteristics.

Feeder type	Screw theoretical volumetric feed rate range (dm^3/h)	Screw speed range (rpm)	Hopper volume (dm^3)
K-PH-ML-KT20	2–200	8–746	12
K-PH-ML-KT35	20–1450	7–556	20

Table 3
List of material characterization methods used during each step of this study, the material properties they measure and corresponding abbreviations of the measured material properties.

Characterization test	Measured property	Abbreviation	Study phase
Ring shear (Brookfield powder flow tester)	Flow function coefficient	FFC	Screening/Optimization/Feeding
Rotating drum (GranuDrum)	Cohesion index	Drum CI	Optimization/Feeding
Stability and variable flow rate (FT4)	Bulk density	Density	Feeding
	Basic Flow Energy	BFE	Feeding
	Specific Energy	SE	Feeding
	Flow rate index	FRI	Feeding
Compression test (FT4)	Compressibility	Compressibility	Feeding
Aeration test (FT4)	Aeration ratio	AR	Feeding
Electrostatic charging (GranuCharge)	Mass charge	Charge	Feeding

addition to the ring shear test flow function coefficient (FFC) during the **optimization study** as the rotating drum allows well comparing powders with similar properties [31]. During the **feeding study**, extended material characterization was performed on the selected optimized blend (from the optimization study) including the different API batches. Table 3 gives an overview of the characterization techniques used during the three parts in this study, as well as the material properties they measure and the corresponding abbreviations of the measured material properties.

2.4.1. Ring shear test

Shear testing was described as a valuable material characterization method during the evaluation and optimization of powder flow and equipment design [30,31], but it is less suitable to distinguish small variations in flow between different powders [32]. The flowability measured via ring shear testing was used to characterize the blends produced during the **screening, optimization** and **feeding studies**. A Brookfield powder flow tester (Brookfield engineering, Harlow, England) was employed to measure the flowability under normal stress. 38 mL of loose powder was poured in the shear cell. The flow function coefficient was measured at five increasing consolidation normal stresses (0.5, 1.1, 2.6, 5.9, 13.2 kPa). Two failure points were measured per consolidation level, respectively 1/3 and 2/3 of the consolidation stress. When the normal stress steady-state was achieved, the shear stress was reduced to zero. The unconfined yield strength (σ_c) and the normal stress (σ_1) were recorded. The slope of the plot σ_1 vs σ_c was the used to calculate the flow function coefficient (**FFC**).

2.4.2. Rotating drum

Limitations of the ring shear test are observed for very cohesive or free-flowing powders at low consolidation stresses. The rotating drum has been described as an efficient complementary test to investigate these specific conditions as it operates under low consolidation stresses [31]. It was consequently used to characterize the formulation blends used in the **optimization** and **feeding studies**. The angle of avalanche is the result of a rotating drum test, providing a measure of the flowability of powder in motion. The angle of avalanche was determined using GranuDrum [29] (GranuTools, Liège, Belgium). A fixed volume of 55 mL of powder was poured into the drum. The angle of avalanche was determined by image analysis at 10 different rotating speeds between 2 and 20 rpm to acquire the flowability profile. 50 images were taken at each rotation speed. On the images, the granular material appears in black while the air appears in white. The position of the air/powder interface is determined by an edge detection. The average interface position and the fluctuations around this average position are computed. From the fluctuations of the interface, the standard deviation is calculated and the corresponding cohesion index (**Drum CI**) is computed. In the case of cohesive powders, the fluctuations of the interface can be very large, making the average angle of avalanche not representative of the material behaviour. The Drum CI representing the amplitude of the fluctuation is then a better indicator of the powder cohesiveness. The measurement was performed in triplicate. The rotating speed presenting the best reproducibility for the Drum CI determination was selected.

2.4.3. Flowability determination using the FT4 powder rheometer

The FT4 powder rheometer (Freeman technology, Tewkesbury, UK) was also used to measure the dynamic flowability. The equipment consists of a measurement vessel in glass and accessories such as blades, pistons and shear heads that can be rotated into a powder sample placed in the vessel whilst axial force and rotational force are measured. More details about the equipment, measurement procedures and calculation of flowability descriptors can be found in a paper from Freeman et al. [33]. For this study, the stability and variable flow rate test was performed with a 160 mL vessel and the 48 mm rotating blade to determine the conditioned bulk density of the powder (**density**), the Basic Flow Energy (**BFE**), the Specific Energy (**SE**) and the Flow Rate Index (**FRI**) of the blends. The aeration test was performed using air flow ranging from 2 to 10 mm/s to determine the aeration ratio (**AR**). The consolidation test was performed at eight pressures with a vented piston between 1 and 15 kPa. The maximum compressibility measured under axial pressure was shown to be equivalent to the Carr index measured via the bulk and tapped density test [34]. Additionally, the densities measured under axial pressure do not suffer from lack of reproducibility due to operator influence, especially for the determination of the bulk density. The volume reduction at 15 kPa (the pressure corresponding to the plateau of volume reduction) was recorded for all tested formulation blends (**Compressibility**). All tests were performed in triplicate for all formulation blends produced at large scale.

2.4.4. Electrostatic charging

Electrostatic charging of powders is known to affect powder flowability [35]. Moreover, powder charge can lead to feeding issues by inducing powder bridging in the hopper or powder accumulation at the outlet of the feeder for instance. The electrostatic charge of the formulation blends produced for the feeding trials was measured using the GranuCharge device (GranuTools, Liège, Belgium). 30 g of each blend was accurately weighted and conditioned at 20 °C, in a room at 60% RH for at least 2 h. The powder was charged by contact with two stainless steel vibrating ramps made of the same stainless steel grade as the feeder. The two ramps were 50 cm long and were connected to each other at a 90° angle. The powder was fed slowly using a vibratory feeder on top of the first ramp to slide along the ramps and was collected in a faraday cup to measure its static charge. The weight of the collected sample was measured to determine the mass charge (**Charge**). All measurements were performed in triplicate.

2.4.5. Scanning electron microscopy

Scanning electron microscopy (SEM) was used to evaluate the presence of agglomerates of API and excipients and excipients coating by colloidal silicon dioxide particles during the **screening** and **optimization studies**. Samples were sputter-coated with gold under vacuum in

an argon atmosphere for 160 s using a Quorum Q150R (Quorum technologies, Laughton, UK). They were then examined in a SEM Jeol JSM-IT300 (Jeol, Zaventem, Belgium) using secondary electron imaging at a distance of 20 mm.

2.5. Data analysis

Partial Least Square (PLS) regression was used to link the formulation blend properties to the feeding behaviour (max. PFR and RSD). PLS models were created using Simca 14.0 software (Umetrics, Umea, Sweden). Two models were built, one for each feeder. For each model, the observations corresponded to the 13 tested blends (five F1 blends and eight F3 blends), the X variables were the nine formulation blends characterization descriptors described in Section 2.4, while the Y variables were the max PFR and RSD of the stability test as described in 2.3.2. Variables were mean centred and scaled to unit variance prior to modelling.

3. Results and discussion

3.1. API batch selection

As outlined in Section 2.1, three API batches were used for the screening study and one API batch was used for the optimization study. All eight API batches were used for the feeding study. During the screening study, it was important to select three API batches covering the entire flowability variability range of all eight API batches. Therefore, the API batches selection for the **screening** and **optimization studies** was done using a previously developed Principal Component Analysis (PCA) model [27]. In a previous study, the data obtained after extensive material characterization (17 API properties including PSD, agglomeration profile, density, flowability, electrostatic charging and surface properties) of the eight API batches was used to create the PCA model explaining the API batch-to-batch variability. The PCA model existed of three principal components (PCs) covering 70.7% (PC1), 14.1% (PC2) and 8.1% (PC3) of the data set variability, respectively. A total of 92.9% of the API batch-to-batch variability was thus explained by the three PCs. The loadings plot shows that the API flowability (e.g., Drum CI, compressibility, BFE; in orange in Fig. 1) contributed almost exclusively to PC1. It was consequently decided to select the API batches from the PC1 versus PC2 scores plot along PC1 (Fig. 2). The extreme API batches (P2/3 and P4/2 in Fig. 2) and an intermediate batch (P1/1 in Fig. 2) were selected for the **screening study** since these three API batches cover the entire API flowability variability. For the **optimization study**, batch P3/1 (Fig. 2) was selected as external batch having intermediate flowability properties.

3.2. Screening study

The aim of the screening study was to compose an alternative formulation to improve the formulation blend flowability. As outlined in Section 2.1.2, the formulation change should respect the composition of the final product. As a consequence, only material transfers from the extra-granular phase to the intra-granular phase were allowed. Three formulations were produced at small scale and tested in terms of flowability (Table 1): the original formulation (F1), a formulation with SMCC transferred to the intra-granular phase (F2) and a formulation with only the glidant (colloidal silicon dioxide) transferred to the intra-granular phase (F3). Herewith, the three API batches (P2/3, P1/1 and P4/2) showing the largest flowability variability were selected and evaluated within each formulation (F1, F2 and F3). Fig. 3 presents the FFC results of the ring shear tests for these three investigated formulations. The API batch-to-batch variability clearly influenced the FFC results of the F1 blends which showed to be very cohesive blends (FFC [1.5–2.5]). Despite the lower API concentration (in the intra-granular phase) in the F2 blends and despite the addition of a well flowable excipient (SMCC) to the intra-granular phase, the flowability was only slightly improved (+0.2) and the same API batch-to-batch variability influence was observed (FFC [1.7–2.7]). The transfer of only the colloidal silicon dioxide to the intra-granular phase (F3) allowed improving the blends flowability (+0.8–1.2) and also reducing the impact of the API batch-to-batch variability on the formulation blend flowability (FFC [2.7–3]). Only API batch P4/2, which has the smallest crystal length and the highest surface area, resulted in lower flowability of blend F3 compared to the two other F3 formulations blends. The formulation with the glidant in the intra-granular phase (F3) hence seemed to be the most promising one to improve the formulation blend flowability and to reduce the impact of the API batch-to-batch variability upon the flowability of the formulation blends.

Two theories have been described by Majerova et al. to explain the improvement of powder flowability caused by glidants [36]. In the first theory introduced, the glidant particles adhere to powder surface, increasing the distance between the particles and leading to reduced adhesive forces. In the second theory, a monolayer of glidant particles is formed on the powder particles, reducing the surface roughness and hence the frictional and adhesive forces. In both theories, the addition

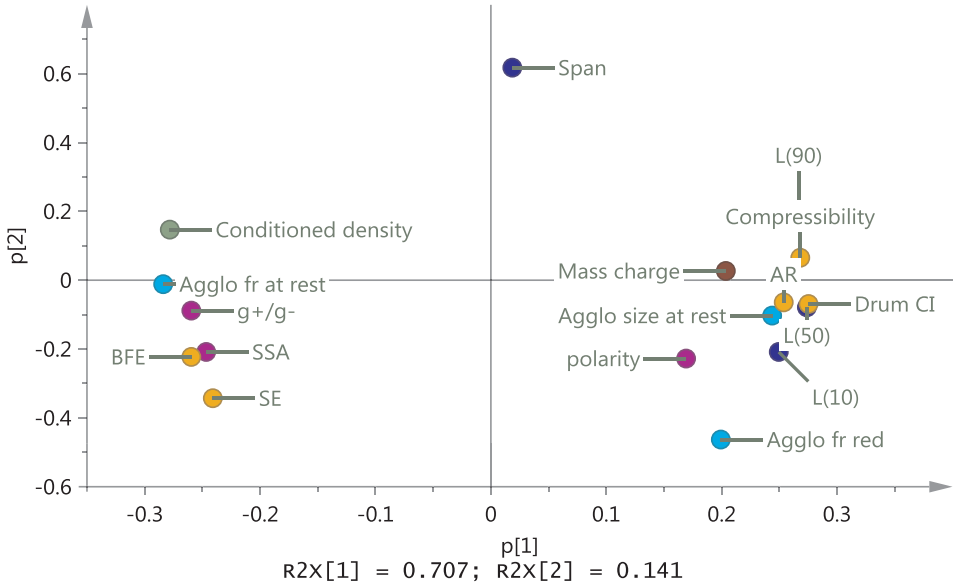

Fig. 1. PC1/PC2 loadings plot - coloured according to properties: in blue: PSD related parameters, in light blue: agglomerate related parameters, in orange: flowability related parameters, in purple: surface related parameters, in red: electrostatic charges, in green: density [27]. (For interpretation of the references to colour in this figure legend, the reader is referred to the web version of this article.)

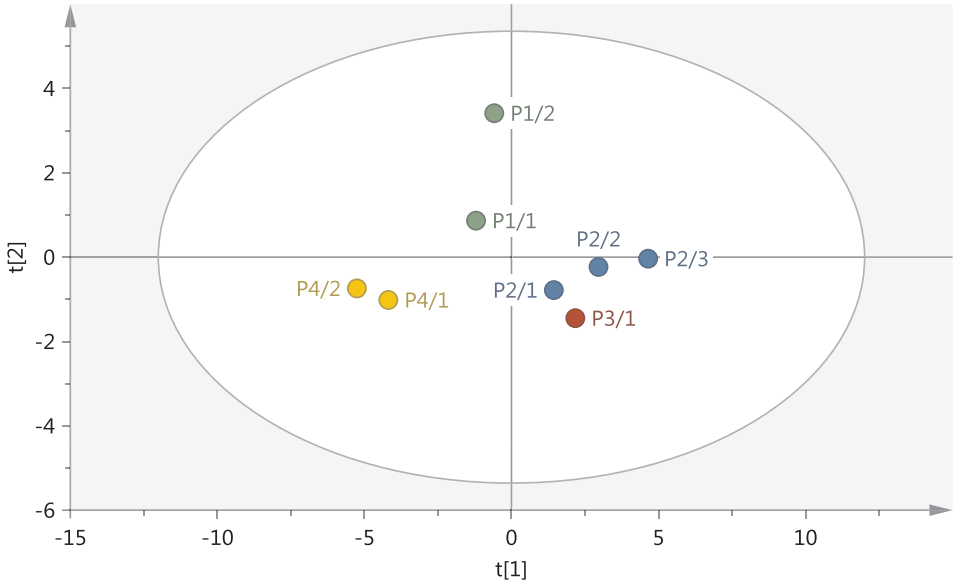

Fig. 2. PC1/PC2 scores plot - coloured according to API crystallization and downstream processes: in green: process 1, in blue: process 2, in red: process 3, in yellow: process 4 [27]. (For interpretation of the references to colour in this figure legend, the reader is referred to the web version of this article.)

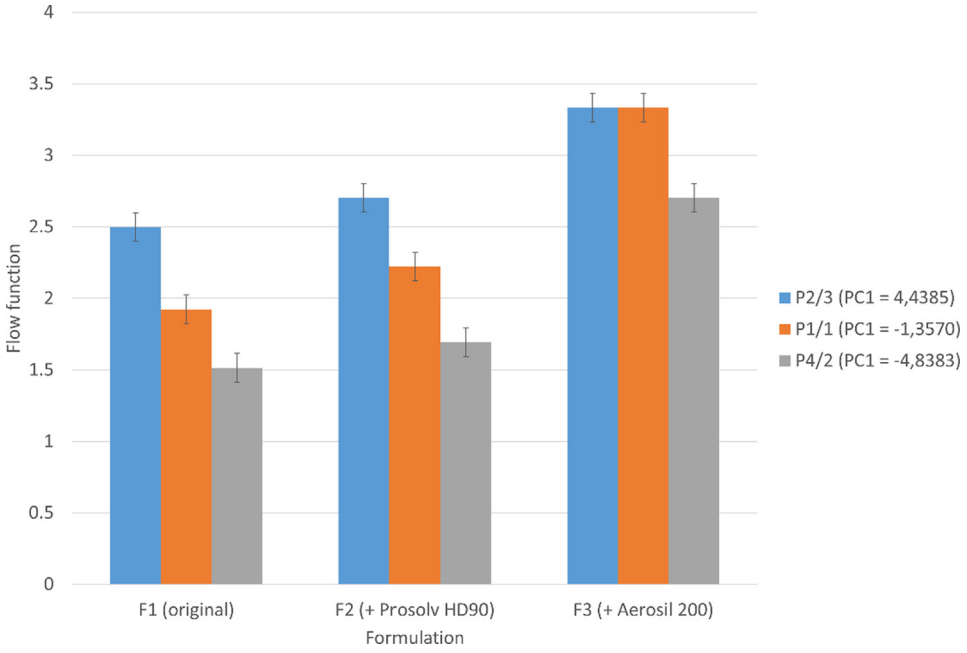

Fig. 3. Comparison of the three tested formulations for the three API batches based on ring shear test. Flow function < 1: not flowing, [1;2]: very cohesive, [2;4]: cohesive, [4;10]: easy-flowing, > 10: free-flowing [36].

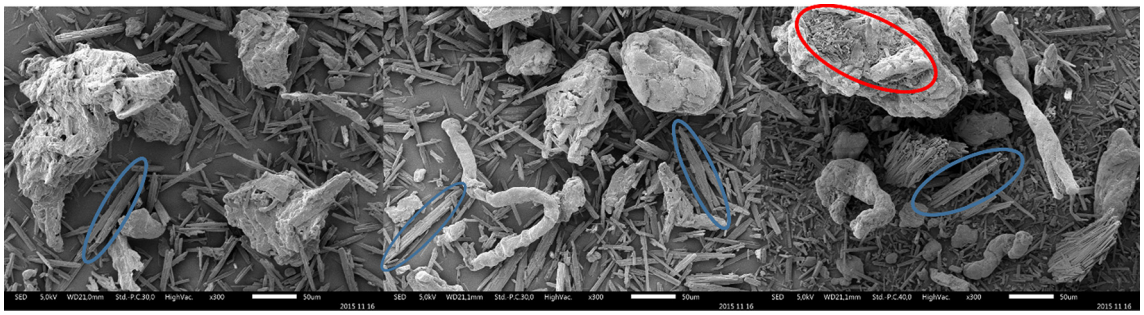

Fig. 4. SEM images of the three formulations produced with API batch P2/3 (×500 – details of the API crystals repartition. Left: F1, centre: F2, right: F3. Needle-shape particles: API crystals, spherical particles: MCC, noodle-shape particles: L-HPC. Blue circles: API agglomerates. Red circle: API crystals spreading on excipient surface. (For interpretation of the references to colour in this figure legend, the reader is referred to the web version of this article.)

of glidant results in a reduction of adhesive forces between the particles. SEM analysis was used to clarify the improved flowability of F3 (Fig. 4). For all three formulation blends, API crystals had the tendency to form agglomerates (blue circles in Fig. 4). SEM analysis showed no clear differences in agglomerate fraction or size between the three tested formulations with no major change in the affinity of API crystals for themselves. However, in F3 blends (Fig. 4 - right picture), the API crystals tended to layer the MCC surface as highlighted by the red circle. As excipients and API particles are coated by silicon dioxide, their surface properties are modified by the presence of the glidant. Cohesion/adhesion forces between API and excipients particle surfaces are therefore modified [37]. As a result, interactions between API and excipient particles became possible (Fig. 4). Due to increased interactions between excipients and API particles, powder packing is improved and blend cohesion is reduced leading to flowability improvement. The flowability improvement was therefore attributed to the reduction in blend cohesion.

No specific difference between the three API batches was observed on SEM analysis. As batch P4/2 exhibited the highest specific surface area, it was suggested that the slightly lower flowability measured for the corresponding F3 blend (Fig. 3 – right plot) might be due to an insufficient concentration of colloidal silicon dioxide to obtain an optimal surface coverage of the API crystals. Moreover, despite the flowability improvement obtained for the F3 blends, the blends are still classified as cohesive by the ring shear test. Further flowability improvement of the F3 blend was then attempted through optimization of the colloidal silicon dioxide grade and its concentration during the optimization study.

3.3. Optimization study

To further optimize the selected formulation (F3), the impact of the colloidal silicon dioxide grade (Aerosil® 200 and 300) and concentration (0.2–1.5%) upon formulation blend flowability was investigated. API batch P3/1 was selected as external batch for the optimization study as having an intermediate flowability according to the PCA model (Fig. 2). Both selected grades of colloidal silicon dioxide were hydrophilic as the intent was to use the blends for wet granulation and differed in terms of surface area (Aerosil® 200: 175–225 m^2/g; Aerosil® 300: 270–330 m^2/g). Fig. 5 presents the change of the FFC results using the ring shear test in function of colloidal silicon dioxide concentration for the two studied grades. No relevant differences between both grades were observed. The flowability strongly increased (1.9–3.1, Fig. 5) by adding colloidal silicon dioxide in concentrations from 0.0% (w/w) to 0.5% (w/w). No further increase in FFC was obtained for concentrations higher than 0.5% (w/w). It was noticed that even the best flowing formulation was still classified as cohesive (FFC [2–4]) and that none of the studied formulations resulted in an easy-flowing blend.

As the ring shear test has been described as poorly discriminant for powders with similar flowability, it was decided to further evaluate the ring shear findings using a more discriminant technique; the rotating drum [31]. Due to the cohesive character of the powder, the cohesion index was used to evaluate the flowability of the blends (see Section 2.4.2 in materials and methods). The value of drum CI measured at 10 rpm was the most reproducible and was therefore used to compare the formulation blends. Contrary to the ring shear results, the rotating drum results identified changes in flowability class (Fig. 6): very poor flow (CI > 55) for blends without 0% (w/w) colloidal silicon dioxide, fair flow ([35; 45]) with 0.2% (w/w) colloidal silicon dioxide, good flow ([25; 35] for 0.5% (w/w) colloidal silicon dioxide, and very good flow (< 25) above 0.8% (w/w) colloidal silicon dioxide (Fig. 6). In contrast, by ring shear testing, no significant improvement in formulation flowability could be measured between 0.5 and 0.8% (w/w) colloidal silicon dioxide. With the rotating drum, a slight flowability improvement was observed for concentrations above 0.5% (w/w), resulting in a change in flowability class. The rotating drum thus seemed to be a more discriminant test than the ring shear to identify flowability changes with similar formulation blends. This observation was also reported by Vasilenko et al. [31]. As powder is consolidated in the shear cell for the ring shear test, the consolidation tends to smooth the differences between similar blends. On the contrary, rotating drum measurements are performed at low stress allowing a better differentiation between similar blends. To conclude, the ring shear test measures the flowability of consolidated powder beds while the rotating drum measures the flowability under low shear. The state of consolidation of the powder showed major differences in terms of result interpretations. The ring shear test allowed evaluating the effect of the formulation change but was not able to discriminate blends prepared with different

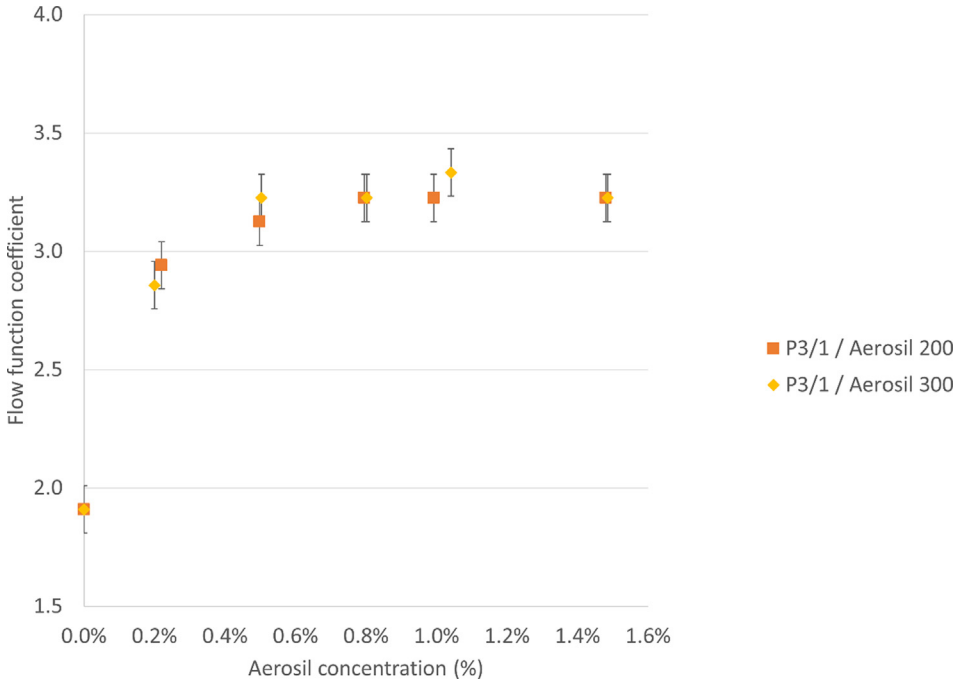

Fig. 5. Impact of the colloidal silicon dioxide grade and its concentration upon the blend flowability (FFC) measured by the ring shear test.

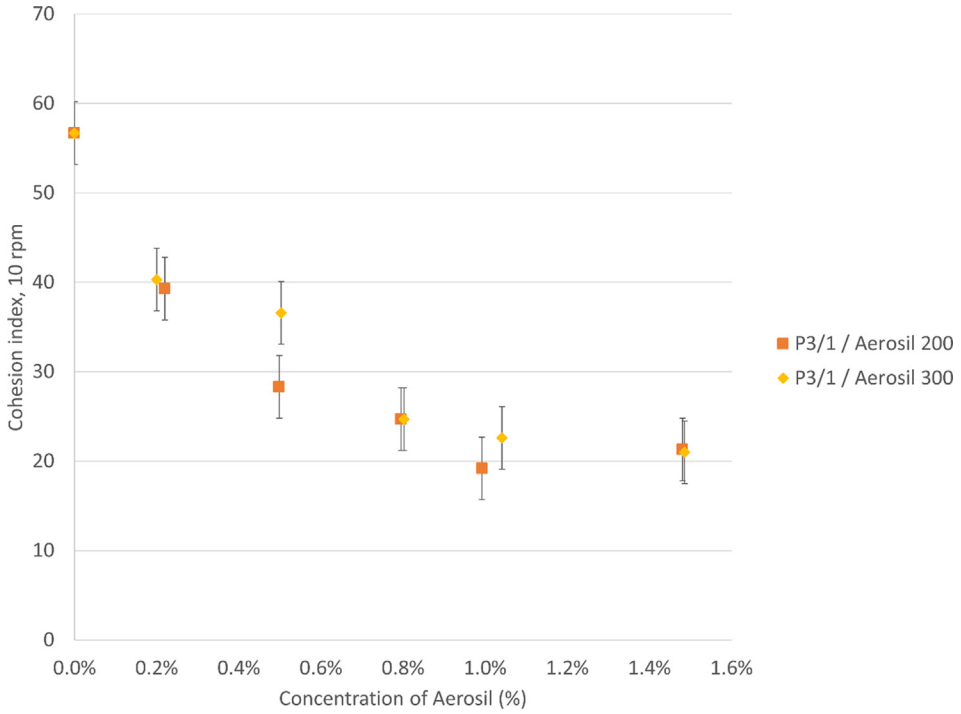

Fig. 6. Impact of the colloidal silicon dioxide grade and its concentration upon the blend flowability (i.e., cohesion index at 10 rpm) measured by the rotating drum.

concentrations of colloidal silicon dioxide. On the other hand, differences in flowability were observed with the rotating drum. A concentration of 0.8% (w/w) of colloidal silicon dioxide was found to be the minimum concentration of colloidal silicon dioxide to achieve the maximum blend flowability (FFC = 3.3, CI = 23).

SEM images showed the API surface coverage by colloidal silicon dioxide (Fig. 7). Even at low concentration (0.2% w/w), the colloidal silicon dioxide (small white grains in Fig. 7) seemed to uniformly cover the API crystals' surface leading to a change in cohesion/adhesion forces between API and excipients and thus explaining the observed improvement of flowability. However, no clear API coverage increase by colloidal silicon dioxide could visually be noticed from 0.2 to 1.5% (w/w) colloidal silicon dioxide.

On the other hand, agglomerates of colloidal silicon dioxide appeared when the highest flowability (FFC = 3.3, CI = 23 for 0.8% w/w) was achieved (red circle in Fig. 8). It was hence concluded that for colloidal silicon dioxide higher than 0.8% (w/w), the glidant did no longer result in increased surface coverage of the API and excipient surface but in colloidal silicon dioxide self-agglomeration. This explains why no improvement in formulation blends flowability was observed for colloidal silicon dioxide concentrations higher than 0.8%.

As no effect of the colloidal silicon dioxide grade was observed, it could be concluded that the specific surface area was not critical within the studied range. Based on this **optimization study**, it was decided to test formulation F1 (original) and the optimized formulation F3 (0.8% w/w Aerosil 200) at larger scale during feeder trials with the eight

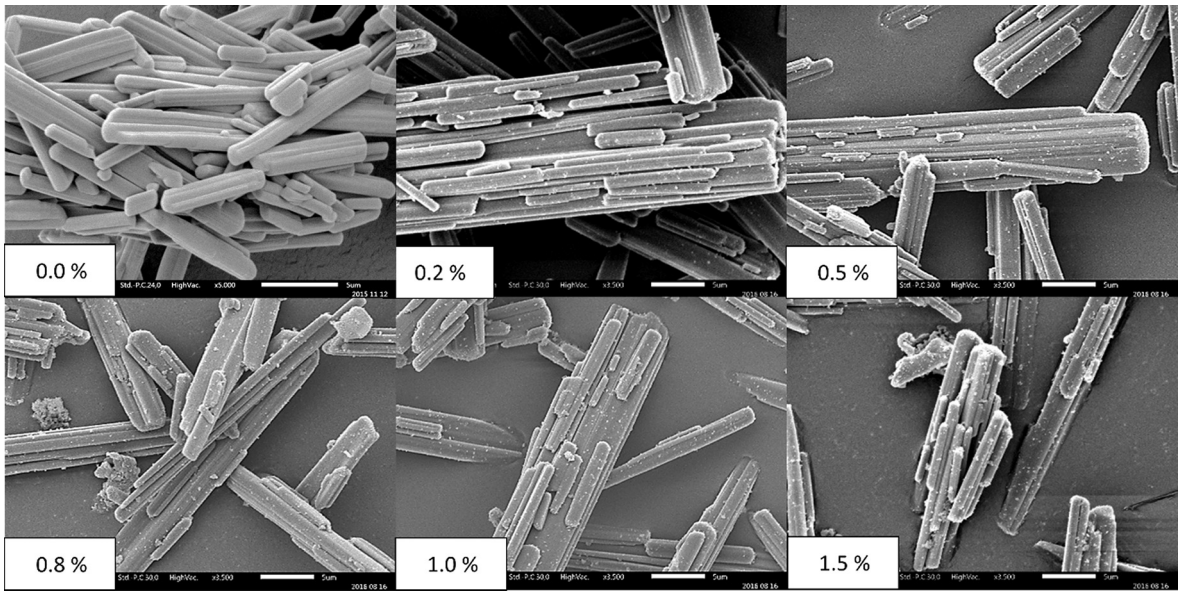

Fig. 7. SEM images of API P3/1 (needle-shape particles) surface covered by colloidal silicon dioxide particles (Aerosil 200, spherical white grains) for formulation blends produced with various concentrations of colloidal silicon dioxide 200 (×3500).

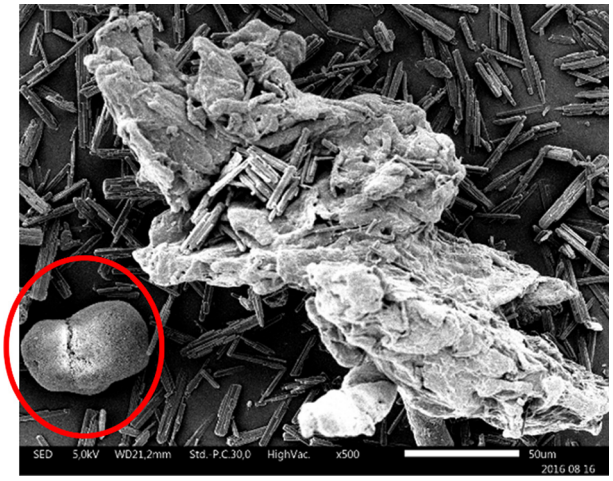

Fig. 8. SEM image of an agglomerate of silicon dioxide (circled in red) for the formulation blend produced with API P3/1 and 0.8% Aerosil® 200 (×500). (For interpretation of the references to colour in this figure legend, the reader is referred to the web version of this article.)

available API batches.

3.4. Feeding study

Formulation blends F1 and F3 were prepared at larger scale for the feeding study (5 kg). Formulation blends F3 were prepared using the eight API batches described in Section 2.1.1. Due to limitations in API availability, formulation blends F1 were prepared using only five of the eight API batches (P1/2, P2/3, P3/1, P4/1 and P4/2, see Fig. 2). Each prepared blend was characterized for flowability and electrostaticity using ring shear tester, rotating drum, FT4 powder rheometer and GranuCharge tester. A feeding evaluation of the formulation blends was performed using a KT20 feeder and a KT35 feeder to evaluate scale-up opportunities, herewith varying the API batches. The blends characterization as well as the feeding characterization results are shown in Table 4.

3.4.1. KT20 feeder evaluation

Firstly, it was observed that the feeding capacities obtained for the F3 blends were generally better and less affected by the API batch (46–53 kg/h, Table 4) compared to the F1 blends (21–51 kg/h, Table 4). It was not even possible to achieve the target feed rate of 25 kg/h with blends F1 P4/1 and F1 P4/2. Therefore it was concluded that the optimized formulation could successfully mitigate the impact of the API batch-to-batch variability upon the feeding capacity due to its improved flowability. The feeding stability (RSD) was similar for the F1 and F3 blends (9.6–15.9%, Table 4), showing no impact of the formulation composition.

In a next step, PLS was used to further clarify the link between the blend material properties, the feeding capacity (max PFR KT20) and the feeding stability (RSD KT20). The five F1 blends and eight F3 blends were used as observations for the model construction. The X-matrix variables consisted of the properties of these blends (density, FFC, Drum CI, BFE, SE, FRI, compressibility, AR and mass charge). The absolute value of the mass charge was used instead of the raw value as the amplitude of the charging is more relevant than the sign of the mass charge. The Y-matrix variables were the max PFR and the RSD. Two PLS1 models predicting max PFR and RSF separately and one PLS2 model predicting both responses simultaneously were built for comparison. With the two responses included in the same model, an R^2X of 82.5%, an R^2Y of 84.5% and a Q^2 of 65.8% were obtained. With the PFR as single response, an R^2X of 84.0%, an R^2Y of 82.5% and a Q^2 of 63.3% were obtained. No improvement in model quality was achieved by having two separate models instead of one. Therefore a single PLS2 model predicting both responses simultaneously was chosen. The developed PLS model consisted of two components explaining respectively 72.9 and 9.6% of the blends characteristics variability (X) and 52.1 and 32.4% respectively of the max PFR variability and RSD (Y).

The bi-plot of the PLS model (Fig. 9) shows the observations (13 formulation blends) as well as their correlations with the X and Y variables (nine characterized properties, the max PFR and the RSD for each blend). Blends from both formulations (F1 in dark red and F3 in orange in Fig. 9) were nicely separated along PLS component 1, demonstrating the impact of the formulation change upon the blend properties and the feeding performances. The batch-to-batch variability due to API batches observed for F1 blends appeared mainly along PLS component 2 (i.e., variability of the F1 observations in the bi-plot). A residual variability was also observed for F3 blends along both PLS components. F3 blends were related to the max PFR, confirming the improved feeding capacity already highlighted in Table 4. The correlations between the max PFR and the blends properties (in green in Fig. 9) allowed explaining the causes of the max PFR improvement for F3 blends. In similar studies investigating a larger range of powder properties, the dominating impact of the bulk density and compressibility upon feeding capacity was highlighted [13,16]. In the present study, the positive correlation between the max PFR and the density and the negative correlation between max PFR and compressibility was also observed. Both properties were found oppositely along PLS component 1. The cluster having negative scores along PLS component 1 comprised drum CI, compressibility, BFE and mass charge. The cluster having positive scores along PLS component 1 included FFC, AR, FRI

Table 4
Results of blends characterization and feeding tests. FFC: flow function coefficient, CI: cohesion index, BFE: Basic flow energy, SE: specific energy, FRI: flow rate index, AR: aeration ratio, PFR: powder feed rate, RSD: residual standard deviation.

Blends	Density (g/ml)	FFC	CI	BFE (mJ/g)	SE (mJ/g)	FRI	Compressibility (%)	AR	Charge (nC/g)	Max PFR KT20 (kg/h)	RSD KT20 (%)	Max PFR KT35 (kg/h)
F1 P1/2	0.23	1.2	61	17.7	10.7	1.46	47	4.53	−6.0	51	12.0	319
F1 P2/3	0.17	1.4	64	14.6	11.4	1.43	55	2.77	−5.3	42	14.5	261
F1 P3/1	0.18	1.1	57	14.0	11.5	1.40	55	2.13	−4.0	32	9.7	226
F1 P4/1	0.23	1.3	49	19.0	13.4	1.32	46	1.23	−5.4	21	N/A	209
F1 P4/2	0.26	1.5	47	21.6	14.8	1.37	39	1.43	−3.8	23	N/A	211
F3 P1/1	0.34	2.0	23	9.4	14.1	3.61	27	5.70	−2.2	53	12.3	379
F3 P1/2	0.36	2.6	21	11.7	14.2	3.19	25	8.78	−2.2	53	11.7	395
F3 P2/1	0.27	2.2	33	9.6	14.1	3.47	33	5.99	−3.9	53	16.0	322
F3 P2/2	0.30	2.8	26	12.1	15.1	3.28	28	12.14	−2.0	48	13.9	318
F3 P2/3	0.29	2.5	25	8.8	11.3	3.60	29	6.08	−1.8	54	15.9	334
F3 P3/1	0.27	2.2	31	10.8	15.8	3.59	31	5.84	−2.3	46	16.8	318
F3 P4/1	0.32	1.8	27	9.2	16.8	3.81	33	6.46	−3.7	47	9.6	351
F3 P4/2	0.33	1.8	28	9.9	16.8	3.70	32	6.74	−3.6	46	11.8	344

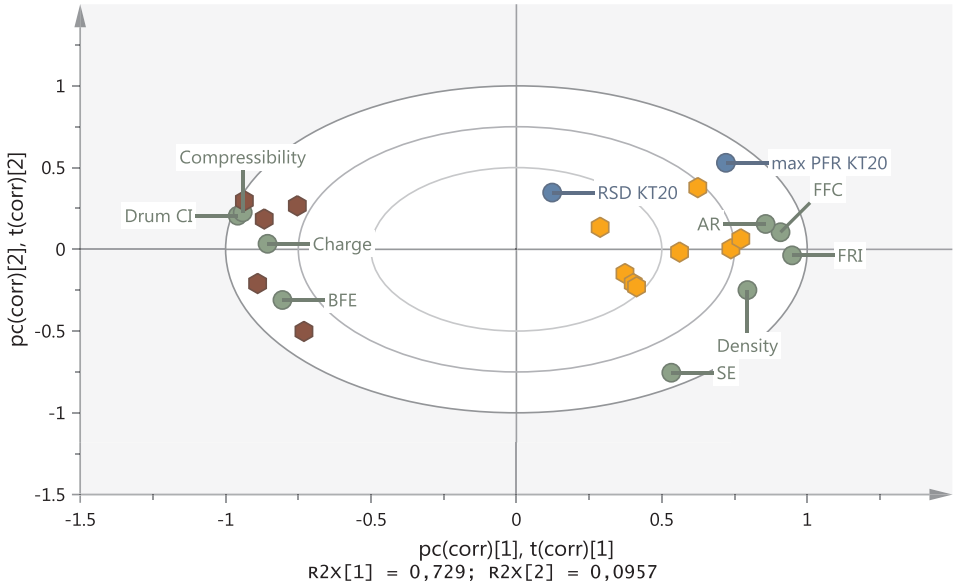

Fig. 9. PC1 versus PC2 bi-plot. In green: blend properties (X-variables), in blue: max PFR KT20 and RSD (Y-matrix variables), in dark red: F1 blends (observations), in orange: F3 blends (observations). (For interpretation of the references to colour in this figure legend, the reader is referred to the web version of this article.)

and blend density. It could hence be concluded that powders with higher density were more sensitive to flow rate changes (FRI) and aeration (AR), less compressible and better flowable (high FFC, low drum CI, low BFE). The mass charge also had an impact on the blend flowability. The electrostatic charging is indeed known to play a major role in powder cohesiveness [35]. During flowability measurements, friction between the powder particles generate electrical charges inducing cohesive forces between the particles. Blends presenting a higher mass charge (expressed in absolute value) were indeed characterized as less flowable (high Drum CI, low FFC, high BFE). The improved feeding capacity was therefore attributed to the higher blend density, the lower electrostatic charging and the resulting better blend flowability. The feeding stability (RSD, in blue in Fig. 9) was displayed in the centre of the plot, showing that its variation was not related to any blend property. The feeding stability (RSD) was indeed similar for all blends (Table 4).

3.4.2. KT35 feeder evaluation

Feeder capacity tests were also performed on a KT35 feeder in order to further evaluate scale-up opportunities. As no specific feed rate was targeted and since the amount of material was too limited to run long feeding experiments at high feed rates, the feeding stability was not evaluated. As observed for KT20, the formulation change (F1 to F3) provided a major improvement in maximum PFR with a slight reduction of the impact of the API batch-to-batch variability (F1 blends: 209–319 kg/h, F3 blends: 318–395 kg/h, Table 4). Considering that the KT35 feeder is planned to be connected to a Consigma 50 granulator, with a usual throughput of 50 kg/h, the max PFR achieved for F1 blends was already very good (209–319 kg/h). As the pitch length of the screws was larger, the material could more easily enter the screws which could explain that the blend cohesiveness was less critical for the feeding capacity. Considering this result, the scale up of feeder could be favoured as alternative to the formulation change to improve the feeding capacity of the F1 blends. However, the large batch-to-batch variability measured for the F1 blends (209–319 kg/h) might have an impact upon the intermediate and final product consistency. When blends properties are changing, for instance after feeder hopper refilling with a new material, the mass flow rate is adapted by the feeder controller to cope with the new blend properties. If the blends properties vary too drastically, the controller could request longer time to adapt the mass flow, leading to potentially inappropriate granule and tablet quality attributes [38]. In addition, KT35 is clearly oversized for the target feed rate (50 kg/h). The feeder would then run at a 10 to 25% of its capacity leading to less accuracy and stability issues. Finally, from an industrial point of view, the integration of a larger feeder in the production line might be a challenge regarding the connections between the feeder and the granulator.

A PLS model was built to unravel the links between the blend characteristics and the feeding capacity (max PFR KT35). The same observations and blends properties were used as for the KT20 PLS model. The Y-vector consisted of the max PFR obtained in the KT35 feeder. A similar PLS model than for the KT20 feeder was obtained, with two PLS components explaining respectively 73.5 and 5.5% of the blend characteristics variability (X) and 69.2 and 23.1% of the max PFR variability (Y). The Q^2 corresponding to the cumulative percentage of model prediction calculated by cross-validation was 69.5% showing a good model prediction. The bi-plot of the PLS model (Fig. 10) showed similar information as for the KT20 feeder. This signifies that the feeding performance on both feeders is influenced by the same blend characteristics. The only difference was that the max PFR was more affected by the blend density on the KT35 as the blend cohesiveness was less critical.

3.5. Perspectives – applications and limitations of the current work

During the **screening** and **optimization studies**, the blends were prepared at small scale (100 g) using a high shear blender, favouring the dispersion of API and colloidal silicon dioxide agglomerates. For the **feeding study**, the blends were prepared at larger scale using a planetary blender bringing less energy into the mixing process. As a result, the blends obtained at larger scale exhibited less flowability compared to the ones prepared at small scale (e.g., FFC 3.3 in Fig. 3 at small scale and 2.2 at larger scale in Table 4). This example showed the impact of the blending scale and blender equipment upon the blend properties. The commercial size of the blending process will be further increased to meet the line throughput requirements of 25 kg/h. Even though formulation F3 exhibited sufficient flowability and a good mitigation of the impact of the API batch-to-batch variability upon the feeding process, the impact of blending scale-up should be kept in mind during future process developments. Thanks to the developed PLS models, it will be possible to evaluate the critical material attributes of the blends to determine whether the produced blends meet the requested powder

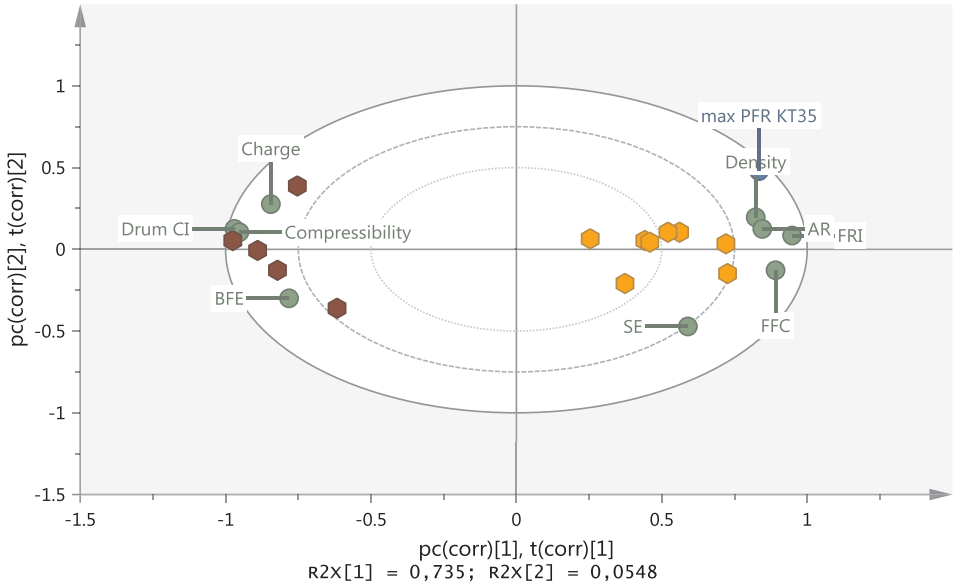

Fig. 10. PC1 versus PC2 bi-plot. In green: blend properties (X-variables), in blue: max PFR KT35 (Y variable), in dark red: F1 blends (observations), in orange: F3 blends (observations). (For interpretation of the references to colour in this figure legend, the reader is referred to the web version of this article.)

feed rate without performing feeding tests. The PLS models could also be updated with new blends in the future to further improve its predictability. As the PLS models are data-driven models, no extrapolation will be possible to predict the feeding capacity of a blend presenting properties outside of the studied range. However, as the largest API variability possible was included in this study, it is most likely that the properties of the new blends will fall within the current range. This also implies that the measurement procedures used for blend characterization need to be kept identical. New characterization tests could also be added to the PLS models through model up-dates.

Finally, in the current study, impact of refilling on feeding stability was not investigated. Feeding stability and its impact upon the downstream process should be further evaluated. Moreover, feeding of a blend could lead to segregation during bin emptying and blend transfer to the feeder. These aspects will have to be investigated during longer runs, taking the ability of the downstream process to dampen the incoming material properties and flow rate variance into account.

4. Conclusion

The goal of this study was to investigate the impact of the batch-to-batch variability of a cohesive API on the feeding capacity of a high drug-load formulation. In order to achieve a sufficient feeding capacity, minor formulation changes were evaluated to improve the flowability of the formulation blend and to mitigate the impact of the API batch-to-batch variability upon the feeding process. Formulation screening and optimization studies were performed at small scale to find the optimal flowability improvement within the pre-defined restrictions (only intra- and extra-granular material could be exchanged). It was found that transferring the glidant from the extra-granular phase to the intra-granular phase was more efficient than API dilution to improve flowability of the formulation blends. Additionally, the formulation change showed a good ability to manage the API batch-to-batch variability as could be observed from blend characterization tests. Feeding trials were then performed to confirm the results obtained at small scale. It was observed that the formulation change allowed to efficiently improve the feeding capacity, but also to mitigate the effect of the API batch-to-batch variability. PLS models showed a clear correlation between blends properties (i.e., density, mass charge, cohesiveness) and the feeding capacity.

Acknowledgments

This work was conducted in the frame of the European Consortium for Continuous Pharmaceutical Manufacturing (ECCPM), funded by the Austrian COMET Program. The authors would like to thank RCPE for their support on the project, Geoffroy Lumay for giving access to GranuTools equipment and advices on the flowability measurements and GEA engineering for their help on feeding tests.

References

[1] C. Vervaet, J. Vercruysse, J.P. Remon, T.D. Beer, Continuous processing of pharmaceuticals, in: Encycl. Pharm. Sci. Technol. Fourth Ed., Taylor & Francis, 2013, pp. 644–655. http://www.tandfonline.com/doi/abs/10.1081/E-EPT4-120050224 (accessed 16.02.15).
[2] S. Byrn, M. Futran, H. Thomas, E. Jayjock, N. Maron, R.F. Meyer, A.S. Myerson, M. P. Thien, B.L. Trout, Achieving continuous manufacturing for final dosage formation: challenges and how to meet them. May 20–21, 2014 Continuous Symposium, J. Pharm. Sci. (2014) n/a-n/a. doi:10.1002/jps.24247.
[3] S.L. Lee, T.F. O'Connor, X. Yang, C.N. Cruz, S. Chatterjee, R.D. Madurawe, C.M.V. Moore, L.X. Yu, J. Woodcock, Modernizing pharmaceutical manufacturing: from batch to continuous production, J. Pharm. Innov. 10 (2015) 191–199, https://doi.org/10.1007/s12247-015-9215-8.
[4] K. Plumb, Continuous processing in the pharmaceutical industry: changing the mind set, Chem. Eng. Res. Des. 83 (2005) 730–738, https://doi.org/10.1205/cherd.04359.
[5] M. Rios, Continuous processing—finally, Pharm. Technol. 31 (2007) 51–53.
[6] A.U. Vanarase, F.J. Muzzio, Effect of operating conditions and design parameters in a continuous powder mixer, Powder Technol. 208 (2011) 26–36, https://doi.org/10.1016/j.powtec.2010.11.038.
[7] Y. Gao, A. Vanarase, F. Muzzio, M. Ierapetritou, Characterizing continuous powder mixing using residence time distribution, Chem. Eng. Sci. 66 (2011) 417–425, https://doi.org/10.1016/j.ces.2010.10.045.
[8] R. Meier, M. Thommes, N. Rasenack, K.-P. Moll, M. Krumme, P. Kleinebudde, Granule size distributions after twin-screw granulation – Do not forget the feeding systems, Eur. J. Pharm. Biopharm. 106 (2016) 59–69, https://doi.org/10.1016/j.ejpb.2016.05.011.
[9] C. Muehlenfeld, M. Thommes, Miniaturization in pharmaceutical extrusion technology: feeding as a challenge of downscaling, AAPS PharmSciTech. 13 (2012) 94–100, https://doi.org/10.1208/s12249-011-9726-7.
[10] W.E. Engisch, F.J. Muzzio, Method for characterization of loss-in-weight feeder equipment, Powder Technol. 228 (2012) 395–403, https://doi.org/10.1016/j.powtec.2012.05.058.
[11] W.E. Engisch, F.J. Muzzio, Loss-in-weight feeding trials case study: pharmaceutical formulation, J. Pharm. Innov. 10 (2014) 56–75, https://doi.org/10.1007/s12247-014-9206-1.
[12] W.E. Engisch, F.J. Muzzio, Feedrate deviations caused by hopper refill of loss-in-weight feeders, Powder Technol. 283 (2015) 389–400, https://doi.org/10.1016/j.powtec.2015.06.001.
[13] J. Dai, J.R. Grace, Biomass granular screw feeding: An experimental investigation,

Biomass Bioenergy 35 (2011) 942–955, https://doi.org/10.1016/j.biombioe.2010.11.026.
[14] Tim Freeman, Doug Millington Smith, Predicting Feeder Performance from Powder Flow Measurements|Powder/Bulk Solids, Powder Bulk Solids, 2015. http://www.powderbulksolids.com/article/Predicting-Feeder-Performance-from-Powder-Flow-Measurements-07-08-2015?page=1 (accessed 17.01.17).
[15] J.K. Prescott, R.A. Barnum, On powder flowability, Pharm. Technol. 24 (2000) 60–84.
[16] J. Falk, R.J. Berry, M. Broström, S.H. Larsson, Mass flow and variability in screw feeding of biomass powders — Relations to particle and bulk properties, Powder Technol. 276 (2015) 80–88, https://doi.org/10.1016/j.powtec.2015.02.023.
[17] Y. Wang, T. Li, F.J. Muzzio, B.J. Glasser, Predicting feeder performance based on material flow properties, Powder Technol. 308 (2017) 135–148, https://doi.org/10.1016/j.powtec.2016.12.010.
[18] J.J. Cartwright, J. Robertson, D. D'Haene, M.D. Burke, J.R. Hennenkamp, Twin screw wet granulation: Loss in weight feeding of a poorly flowing active pharmaceutical ingredient, Powder Technol. 238 (2013) 116–121, https://doi.org/10.1016/j.powtec.2012.04.034.
[19] M.D. Parker, P. York, R.C. Rowe, Binder-substrate interactions in wet granulation. 3: The effect of excipient source variation, Int. J. Pharm. 80 (1992) 179–190, https://doi.org/10.1016/0378-5173(92)90276-8.
[20] A. Hagsten, C. Casper Larsen, J. Møller Sonnergaard, J. Rantanen, L. Hovgaard, Identifying sources of batch to batch variation in processability, Powder Technol. 183 (2008) 213–219, https://doi.org/10.1016/j.powtec.2007.07.042.
[21] M. Fonteyne, H. Wickström, E. Peeters, J. Vercruysse, H. Ehlers, B.-H. Peters, J.P. Remon, C. Vervaet, J. Ketolainen, N. Sandler, J. Rantanen, K. Naelapää, T.D. Beer, Influence of raw material properties upon critical quality attributes of continuously produced granules and tablets, Eur. J. Pharm. Biopharm. 87 (2014) 252–263, https://doi.org/10.1016/j.ejpb.2014.02.011.
[22] M. Fonteyne, A. Correia, S. De Plecker, J. Vercruysse, I. Ilić, Q. Zhou, C. Vervaet, J.P. Remon, F. Onofre, V. Bulone, T. De Beer, Impact of microcrystalline cellulose material attributes: A case study on continuous twin screw granulation, Int. J. Pharm. 478 (2015) 705–717, https://doi.org/10.1016/j.ijpharm.2014.11.070.
[23] M.G. Herting, P. Kleinebudde, Roll compaction/dry granulation: Effect of raw material particle size on granule and tablet properties, Int. J. Pharm. 338 (2007) 110–118, https://doi.org/10.1016/j.ijpharm.2007.01.035.
[24] J. Kushner IV, B.A. Langdon, J.I. Hiller, G.T. Carlson, Examining the impact of excipient material property variation on drug product quality attributes: a quality-by-design study for a roller compacted, immediate release tablet, J. Pharm. Sci. 100 (2011) 2222–2239, https://doi.org/10.1002/jps.22455.
[25] J. Albers, K. Knop, P. Kleinebudde, Brand-to-brand and batch-to-batch uniformity of microcrystalline cellulose in direct tableting with a pneumohydraulic tablet press, Pharm. Ind. 68 (2006) 1420–1428.
[26] G. Thoorens, F. Krier, E. Rozet, B. Carlin, B. Evrard, Understanding the impact of microcrystalline cellulose physicochemical properties on tabletability, Int. J. Pharm. 490 (2015) 47–54, https://doi.org/10.1016/j.ijpharm.2015.05.026.
[27] F. Stauffer, V. Vanhoorne, G. Pilcer, P.-F. Chavez, S. Rome, M.A. Schubert, L. Aerts, T. De Beer, Raw material variability of an active pharmaceutical ingredient and its relevance for processability in secondary continuous pharmaceutical manufacturing, Eur. J. Pharm. Biopharm. 127 (2018) 92–103, https://doi.org/10.1016/j.ejpb.2018.02.017.
[28] A. Kumar, M. Alakarjula, V. Vanhoorne, M. Toiviainen, F. De Leersnyder, J. Vercruysse, M. Juuti, J. Ketolainen, C. Vervaet, J.P. Remon, K.V. Gernaey, T. De Beer, I. Nopens, Linking granulation performance with residence time and granulation liquid distributions in twin-screw granulation: An experimental investigation, Eur. J. Pharm. Sci. (n.d.). 10.1016/j.ejps.2015.12.021.
[29] G. Lumay, F. Boschini, K. Traina, S. Bontempi, J.-C. Remy, R. Cloots, N. Vandewalle, Measuring the flowing properties of powders and grains, Powder Technol. 224 (2012) 19–27, https://doi.org/10.1016/j.powtec.2012.02.015.
[30] D. Schulze, Shear testing of powders for process optimization, Annu. Trans. Nord. Rheol. Soc. 21 (2013) 99–106.
[31] A. Vasilenko, B.J. Glasser, F.J. Muzzio, Shear and flow behavior of pharmaceutical blends — Method comparison study, Powder Technol. 208 (2011) 628–636, https://doi.org/10.1016/j.powtec.2010.12.031.
[32] M. Leturia, M. Benali, S. Lagarde, I. Ronga, K. Saleh, Characterization of flow properties of cohesive powders: A comparative study of traditional and new testing methods, Powder Technol. 253 (2014) 406–423, https://doi.org/10.1016/j.powtec.2013.11.045.
[33] R. Freeman, Measuring the flow properties of consolidated, conditioned and aerated powders—a comparative study using a powder rheometer and a rotational shear cell, Powder Technol. 174 (2007) 25–33, https://doi.org/10.1016/j.powtec.2006.10.016.
[34] M. Li, Study of the FT4 powder rheometer: comparison of the test methods and optimization of the protocols, UTC Compiègne, 2017.
[35] K.C. Pingali, T. Shinbrot, S.V. Hammond, F.J. Muzzio, An observed correlation between flow and electrical properties of pharmaceutical blends, Powder Technol. 192 (2009) 157–165, https://doi.org/10.1016/j.powtec.2008.12.012.
[36] D. Majerová, L. Kulaviak, M. Růžička, F. Štěpánek, P. Zámostný, Effect of colloidal silica on rheological properties of common pharmaceutical excipients, Eur. J. Pharm. Biopharm. 106 (2016) 2–8, https://doi.org/10.1016/j.ejpb.2016.04.025.
[37] S. Jonat, S. Hasenzahl, A. Gray, P.C. Schmidt, Mechanism of glidants: Investigation of the effect of different colloidal silicon dioxide types on powder flow by atomic force and scanning electron microscopy, J. Pharm. Sci. 93 (2004) 2635–2644, https://doi.org/10.1002/jps.20172.
[38] J. Winski, The cause of loss-in-weight feeder performance problems? Process, Mag, 2016 (accessed April 22, 2016).